Disrupting actin filaments enhances glucose-stimulated insulin secretion independent of the cortical actin cytoskeleton

Alexander J. Polino, Xue Wen Ng, Rebecca Rooks, and David W. Piston*
From the Department of Cell Biology & Physiology, Washington University School of Medicine, St Louis, Missouri, USA

Reviewed by members of the JBC Editorial Board. Edited by Enrique De La Cruz

Just under the plasma membrane of most animal cells lies a dense meshwork of actin filaments called the cortical cytoskeleton. In insulin-secreting pancreatic β cells, a long-standing model posits that the cortical actin layer primarily acts to restrict access of insulin granules to the plasma membrane. Here we test this model and find that stimulating β cells with pro-secretory stimuli (glucose and/or KCl) has little impact on the cortical actin layer. Chemical perturbations of actin polymerization, by either disrupting or enhancing filamentation, dramatically enhance glucose-stimulated insulin secretion. Using scanning electron microscopy, we directly visualize the cortical cytoskeleton, allowing us to validate the effect of these filament-disrupting chemicals. We find the state of the cortical actin layer does not correlate with levels of insulin secretion, suggesting filament disruptors act on insulin secretion independently of the cortical cytoskeleton.

Most animal cells are enveloped in a dense layer of actin filaments called the cortical cytoskeleton. In coordination with myosins and other actin-binding proteins, this layer is dynamically remodeled, driving cell shape changes required for motility, division, and contractile tissue motion (1). In models of regulated secretion, the cortex has been implicated in two opposing functions. First, the dense cortical network restricts access of secretory granules to the plasma membrane. Second, cortex remodeling enables secretion by providing a path to secretory sites and generating force to complete granule fusion with the plasma membrane (2, 3).

In pancreatic β cells, cortical actin has been hypothesized to primarily restrict the access of insulin granules to the plasma membrane, limiting insulin secretion. This model rests on the observations that stimulating β cells with pro-secretory levels of glucose dramatically reduces levels of total cellular actin (4–8), and that forcing the depolymerization of the actin cortex with chemical disruptors enhances glucose-stimulated insulin secretion (GSIS) (9–11). The first finding has been shown in immortalized β cell models INS-1 (4) and MIN6 (5) as well as in *ex vivo* murine islets (8). However, various reports have found inconsistent results, ranging from no change in

actin staining to over 50 percent loss of actin staining. The second finding was originally shown in Lelio Orci's 1972 electron microscopy study describing cortical microfilaments in the β cells of rat islets; a 90-min treatment with the actin depolymerizer cytochalasin B enhanced GSIS from rat islets by around 50% (10). This finding has since been recapitulated in dispersed and intact mouse islets with a variety of chemicals and concentrations (8, 9, 11). Curiously, pretreatment with the filament polymerizing drug jasplakinolide also enhanced GSIS in MIN6 (12) and mouse islets (11), phenocopying filament disruptors. This finding seems at odds with the model of cortical actin restricting granule secretion.

Here, we sought to test the model of cortical actin restricting insulin secretion by investigating each of its supporting observations with fluorescence and scanning electron microscopy, correlated with secretion assays. We find that glucose or KCl stimulation has only minimal impact on the density of cortical actin filaments, both in MIN-6 cells and mouse pancreatic islets. Further, we find that modulating the actin filament structure by chemical inhibition of filament formation or stabilization of actin polymerization both dramatically enhance glucose-stimulated insulin secretion. Thus, the state of the cortical cytoskeleton does not explain the shared phenotype of actin disruption enhancing insulin secretion. Instead, our data support a model where the effect of actin filament disruption on insulin secretion is independent of the cortical cytoskeleton.

Results

Stimulating β cells does not substantially change actin levels

We sought to expand upon prior observations by investigating actin levels at various times after stimulating β cells with glucose or KCl. Throughout this work, 11 mM glucose is used to stimulate *ex vivo* mouse islets nd 20 mM glucose to stimulate the immortalized murine β cell model MIN6. In all, 30 mM KCl is used as an alternative secretagogue, as it directly depolarizes the plasma membrane, resulting in secretion independent of the canonical glucose sensing pathway. To quantify F-actin levels, we stimulated MIN6 cells or murine islets with high glucose or high glucose plus KCl. We then fixed the samples at 0, 2, 5, 10, or 15 min after stimulation, stained the F-actin with phalloidin-

---

* For correspondence: David W. Piston, piston@wustl.edu.

Cortical actin and insulin secretion

AlexaFluor488, and imaged at the cell-coverslip boundary, where actin networks are most prominent. F-actin levels were quantified per cell area (Fig. 1, *A* and *B*) or per islet area (Fig. 1, *C* and *D*). We find only slight changes in global actin levels in stimulated MIN6 cells (one-way ANOVA, $F_{(8, 149)} = 2.138$, $p = 0.0356$). Most group means vary by just a few percent from the unstimulated control. Dunnett's multiple comparisons test shows that the only statistically significant difference is between control and 10-min glucose + KCl treatment (adjusted *p*-value of 0.0109, and a 95% confidence interval of the magnitude of difference ranging from 0.02150 to 0.2384). Murine islets have more natural variation in size

and actin staining than MIN6 cells but still fail to show a consistent effect of pro-secretory stimuli on actin levels (one-way ANOVA, $F_{(8, 130)} = 3.021$, $p = 0.0038$). Again, Dunnett's multiple comparisons indicate that the only statistically significant difference is between control and 10-min glucose treatment (adjusted *p*-value of 0.0067, and a 95% confidence interval of the difference ranging from 0.067 to 0.602). Given that the direction of change is opposite that seen in the MIN6 cells, not seen at other time points or in KCl-treated islets, and opposite of that described in prior literature, we suspect it is just an outlier as a result of biological variation of *ex vivo* islets, and not physiologically relevant.
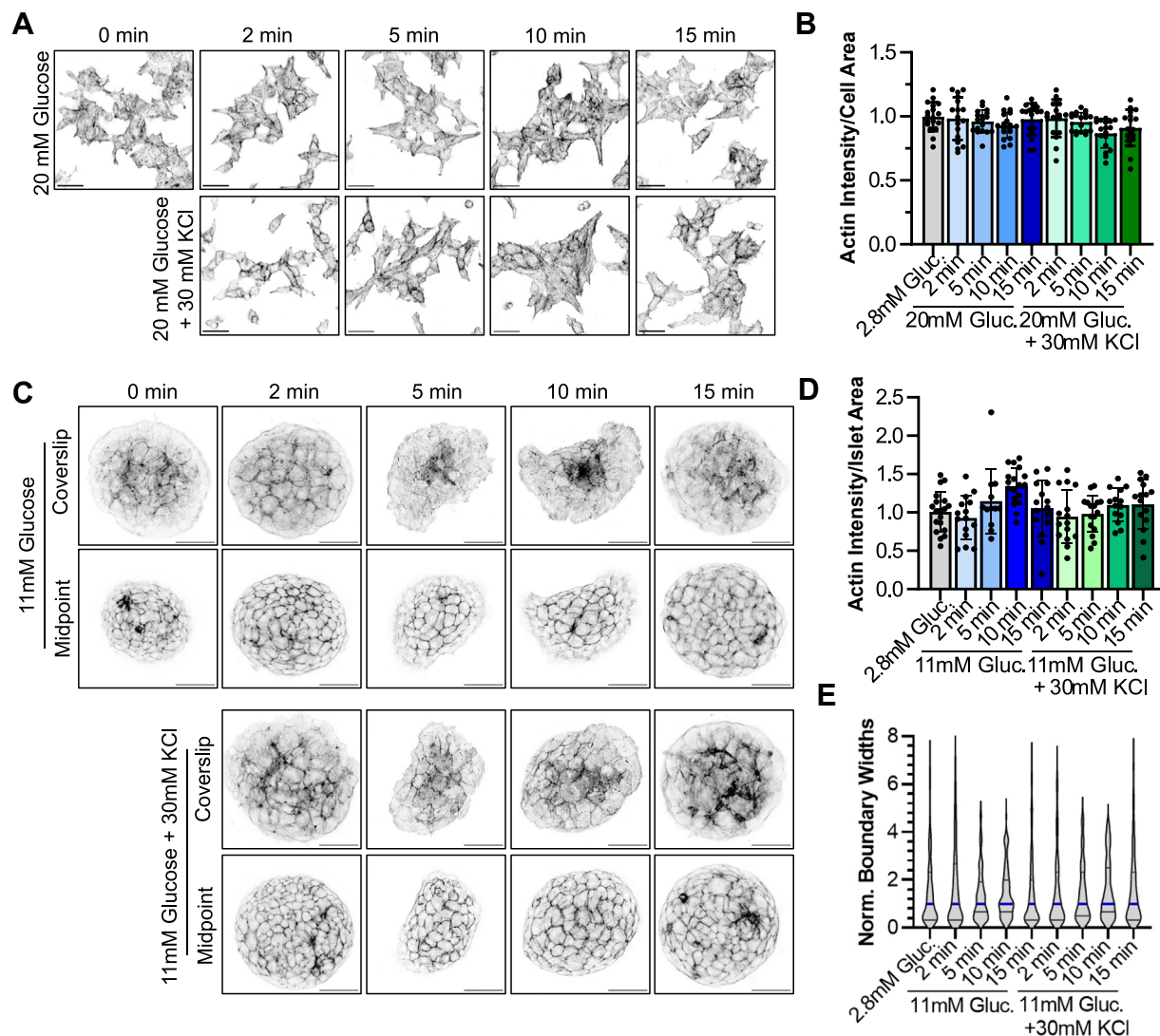

Figure 1. Stimulating β cells does not substantially change actin levels. *A*, MIN6 cells were stimulated with high glucose (20 mM) ± 30 mM KCl and fixed at 0, 2, 5, 10, or 15 min. Actin in fixed cells was stained with phalloidin-AlexaFluor488, and imaged. Representative images are shown. Scale bars represent 20 μm. *B*, graph comparing the actin intensity per cell area for each image. The experiment was performed three times, with six images quantified per condition in each experiment. All points are shown, each representing the actin intensity for a given image; error bars represent standard deviation. *C*, islets stimulated as in (*A*) with high glucose (11 mM) ± 30 mM KCl and fixed at times indicated. Each islet was imaged at the coverslip (*upper row*) to highlight actin networks at the coverslip interface, and at its midpoint (*lower row*) to highlight actin at cell-cell boundaries. Scale bars represent 40 μm. *D*, actin intensity was quantified per islet area. Experiment was performed three times with up to six islets imaged each time. All points are shown, each representing the actin intensity divided by a given islet's area; error bars represent standard deviation. *E*, the breadth of actin staining at cell-cell boundaries was measured from two perpendicular lines through five islets per condition. The *thick blue line* represents the median of the measured boundaries, and the *thin black lines* the first and third quartiles.

We also quantified the F-actin signal by acquiring confocal images through the middle of each islet (Fig. 1C, "Midpoint") where the phalloidin signal corresponds primarily to the cortical actin ring around each cell. We measured the widths of these cell-cell boundaries, which again exhibit no substantial differences between treatment groups (Fig. 1E, Kruskal-Wallis test, p = 0.6682). As a verification of the fluorescence measurements of F-actin, we also quantified actin filamentation biochemically in MIN6 following stimulation for 5 min, as shown to stimulate actin rearrangements in prior reports (5, 8). We lysed the cells and separated intact actin filaments by ultracentrifugation. We detect no effect of glucose ± KCl on the global actin filament state (Fig. S1).

Cortical actin is a meshwork of filaments, with filaments too densely packed to be resolved by light microscopy. To image directly the effects of glucose/KCl stimulation on finer cortex architecture, we fixed MIN6 cells or mouse islets, detergent-extracted the plasma membranes, and used scanning electron microscopy (SEM) to visualize the cytoskeleton (Fig. 2). Consistent with the fluorescence and biochemical assays, we see no global change in cortical cytoskeleton arrangement after pro-secretory stimulation either in MIN6 cells (Fig. 2, A and B) or islets (Fig. 2, C and D). Quantifying the percentage of the cell surface covered by filaments reveals no change with stimulation in MIN6 cells (one-way ANOVA, $F_{(2, 33)}$ = 1.215, p = 0.3097), and a slight increase in coverage with islet stimulation (one-way ANOVA, $F_{(2, 51)}$ = 22.64, $p < 0.0001$) of a magnitude less than 10% (Fig. 2, B and D).

Actin filament-disrupting drugs enhance GSIS

We next sought to expand upon the previous observation that actin-depolymerizing agents enhance GSIS. We recapitulate this observation, finding that a 30-min pre-treatment with actin depolymerizers enhances GSIS in a concentration-dependent manner. This is true for filament barbed-end binders cytochalasin B and D (Fig. 3, A and B), filament pointed-end binders latrunculins A and B (Fig. 3, C and D), and the filament-severing drug swinholide A (Fig. 3E). This is also consistent across both MIN6 cells (Fig. 3, A–E), and mouse islets (Fig. 3F). Surprisingly, we see a similar dose-dependent enhancement of GSIS in cells or islets pre-treated with the filament-enhancing drug jasplakinolide (Fig. 4). This raises the question: why do compounds with seemingly opposite effects on actin have the same effect on insulin secretion?

Actin cortex state does not explain insulin secretion phenotype

To determine if these drugs were acting by some shared effect on the cortical actin architecture, we again employed SEM on membrane-stripped mouse islets pre-treated with
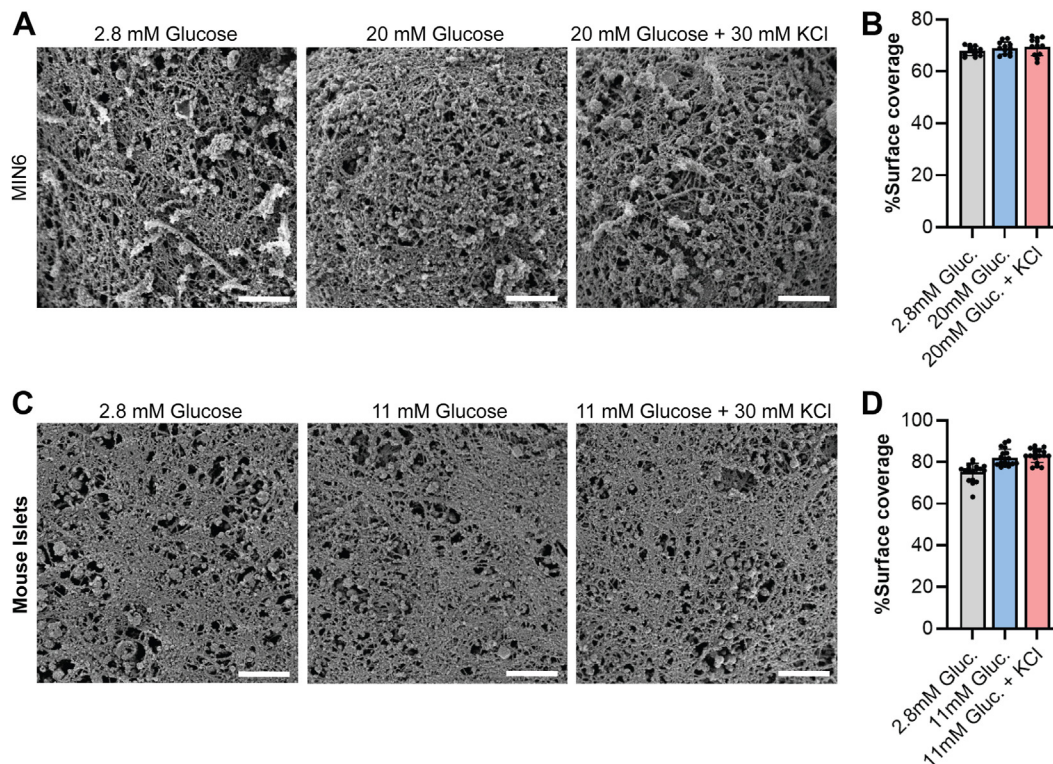

Figure 2. Stimulating β cells does not dramatically change the actin cortex. *A*, SEM images of membrane-stripped MIN6 cells revealing the cortical cytoskeleton. Cells were treated with 2.8 mM glucose, 20 mM glucose, or 20 mM glucose +30 mM KCl for 5 min prior to fixation and membrane stripping. Scale bars represent 1 μm. *B*, the percent of the surface covered by the cytoskeleton was quantified in 10 to 12 images per condition. Error bars represent standard deviations. *C*, mouse islets are treated as above, but with 2.8 mM glucose, 11 mM glucose, or 11 mM glucose +30 mM KCl. Scale bars represent 1 μm. *D*, six images from each of the three islets were quantified per condition, as in (*B*). Error bars represent standard deviation. This experiment was performed twice with similar results. The results from one experiment are shown above. Zoomed-out images are provided in Figure 2.

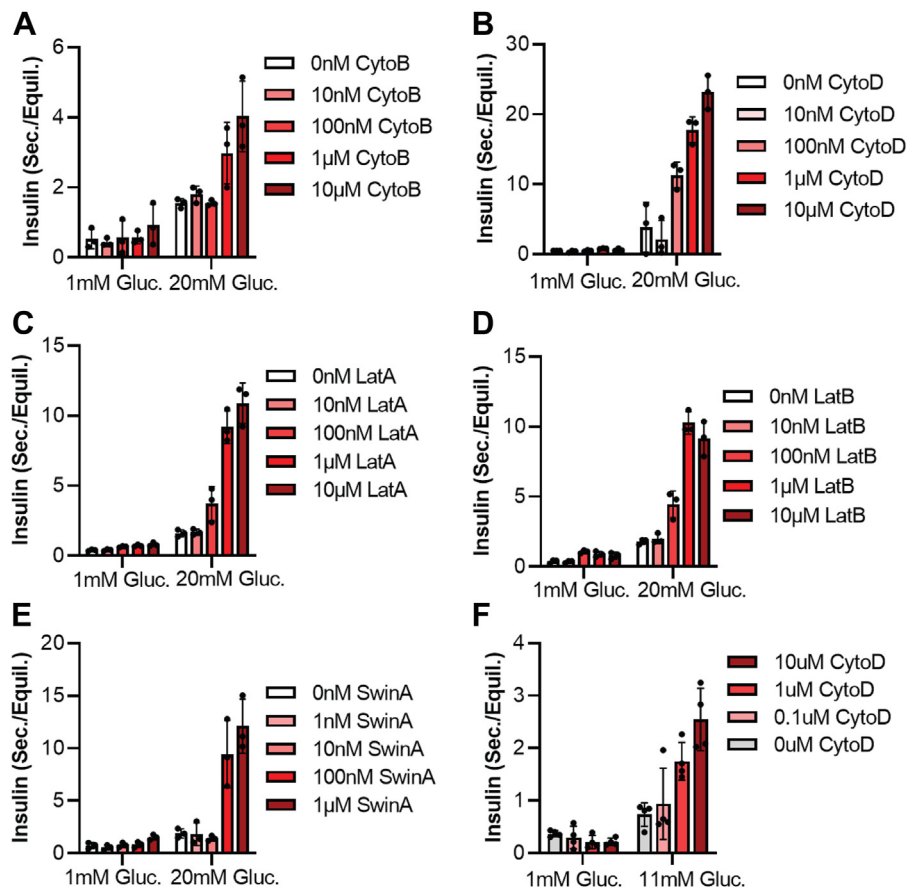SASBMB

J. Biol. Chem. (2023) 299(11) 105334 **3**

Figure 3. Actin filament disruptors enhance GSIS at all concentrations. *A–E*, insulin secretion assay from MIN6 cells. Cells were equilibrated for an hour in KRBH +2.8 mM glucose ("Equil."), pre-treated in KRBH +2.8 mM glucose + the indicated inhibitor concentration, then treated with high (20 mM) or low (1 mM) glucose with the indicated amounts of inhibitor for 1 h ("Sec."). Points represent the amount of insulin in the "Sec." sample of a given well divided by the amount of insulin in the "Equil." sample from the same well. Three wells were tested per condition, with the insulin from each measured in technical duplicate. Each point represents the average of the technical duplicates from a single well. Bar height represents the mean of the three wells; error bars the standard deviation. Experiments were performed three times; a representative replicate of each is shown. *F*, insulin secretion assay from mouse islets. Four islets per well; four wells per condition. Otherwise as above. Inhibitors are the actin filament disruptors cytochalasin B (CytoB), cytochalasin D (CytoD), latrunculin A (LatA), latrunculin B (LatB), and swinholide A (SwinA).

the actin depolymerizers cytochalasin D and latrunculin B, as well as the actin filament enhancer jasplakinolide (Fig. 5). Directly visualizing the cortical cytoskeleton in this way allows us to unequivocally determine the effect of these filament-disrupting compounds on the steady state cortical architecture. Without a drug, the actin cortex provides dense cover across the cell surface. Cytochalasin D or latrunculin B treatment dramatically strips away the topmost actin layer, revealing a network of thicker filaments and vesicles beneath. In contrast, after jasplakinolide treatment, the cortical cytoskeleton remains at least as dense as without the drug. Thus, after drug treatment the cortical cytoskeleton state is discordant with the insulin secretion phenotype, suggesting these compounds do not enhance insulin secretion by modulating the cortical cytoskeleton density.
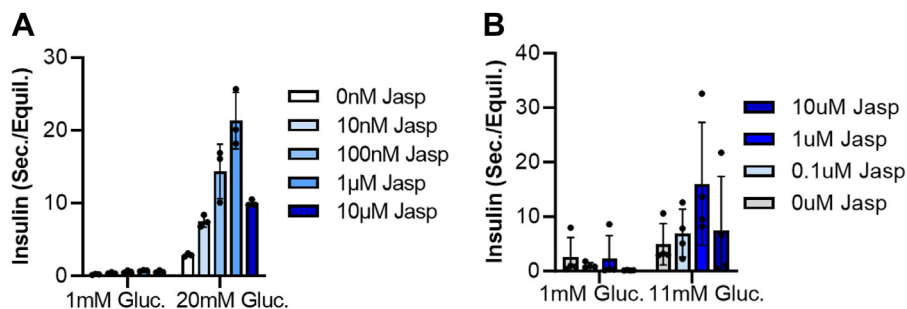

Figure 4. Actin filament-supporting drug also enhances GSIS at all concentrations. Insulin secretion assays from (*A*) MIN6 cells and (*B*) mouse islet. Done exactly as in Figure 3. Jasplakinolide (Jasp).
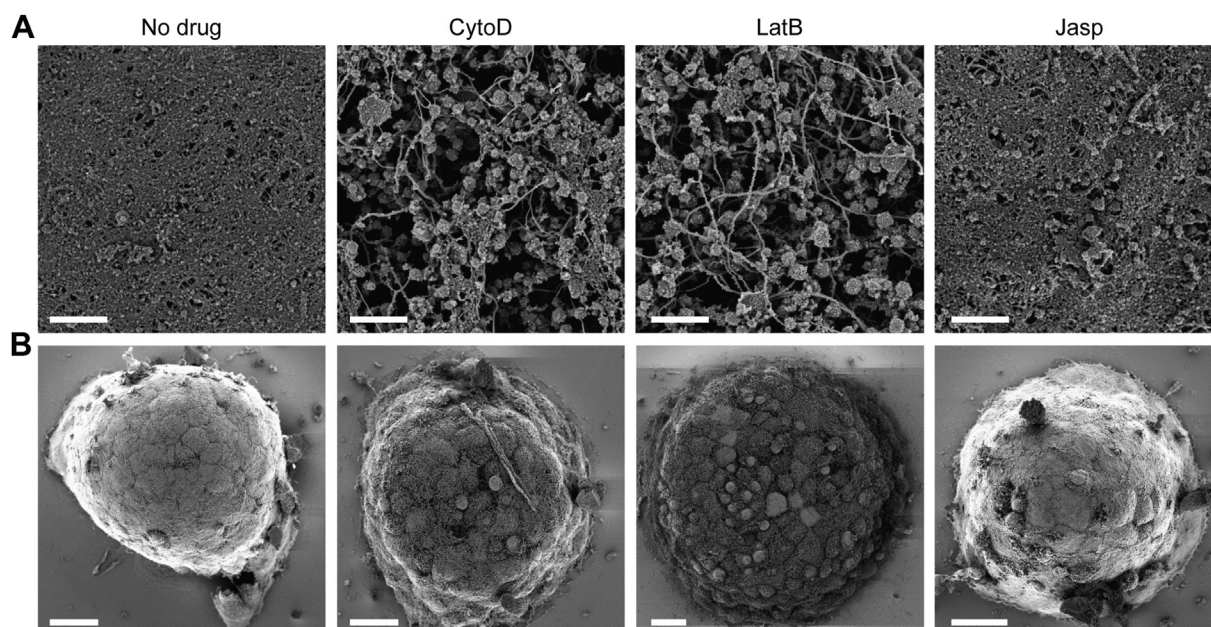
Figure 5. Cytoskeleton-modifying drugs that enhance GSIS have opposite effects on the cortical cytoskeleton. *A*, mouse islets were treated for 30 min with KRBH plus 2.8 mM glucose (KRBH), or the same plus 1 µM cytochalasin D (CytoD), 1 µM latrunculin B (LatB), or 1 µM jasplakinolide (Jasp). Islets were then fixed, membranes extracted, and surfaces imaged by SEM as in Figure 2. Images are shown at 12,000× zoom. Scale bars represent 1 µm. *B*, zoomed-out images of islets from the same samples. Scale bars represent 20 µm. The experiment was performed twice with similar results; representative images are shown. More uncropped images are shown in Figure 3.

Discussion

We set out to investigate the relationship between the cortical actin cytoskeleton and insulin secretion, testing a variety of compounds, concentrations, and treatment times toward unifying the apparently conflicting reports in the literature. We find that pro-secretory stimuli have little effect on the density of the cortical actin network. Further, we find drugs that disrupt or enhance actin filament formation both enhance GSIS, by a mechanism that is not directly tied to cortical cytoskeleton density. While these data suggest that the drugs are not affecting insulin secretion directly *via* the cortical cytoskeleton, the mechanism that ties cortical actin perturbation to modified GSIS remains to be elucidated.

Our finding that stimulation causes little-to-no change in the actin cytoskeleton matches a recent study of dispersed mouse islets (9) but stands in contrast to several past studies (4–6, 8). We have attempted to recapitulate the conditions used in these studies, matching the treatment conditions and times to the extent possible. Perhaps in some conditions, we were unable to account for, for example, mouse/cell line genetics, cell density, or some unreported element of the media or substrate; this explains the difference between our findings and others. However, in our hands, cells, and islets secrete insulin in response to glucose or KCl without substantially degrading their actin cytoskeletons, suggesting the actin degradation that other groups have reported is not required for insulin secretion. It remains possible that our time course fails to capture moments of transient rearrangement, or that meaningful changes in the actin cortex are not preserved in fixed cells. Both of these possibilities could be investigated by live microscopy in the future. Alternatively, dramatic actin

rearrangement may occur only at sites of granule fusion, a model supported by Ma, *et al.* (2020) who describe "flashes" of Lifeact-GFP at sites of vesicle fusion. Given the small size of insulin granules (∼400 nm across), tracking these changes in real time and at high resolution may require further technical advances in live microscopy. We find that pre-treatment of MIN6 cells or mouse islets with filament disruptors or enhancers potentiates GSIS as previously shown (11). We extend this previous work by showing that this phenomenon is not unique to a particular actin-modifying compound or concentration, but is the case for several compounds in a concentration-dependent manner.

Why should these two classes of compounds with seemingly opposite effects on actin have the same effect on GSIS? We see two possibilities. (1) The two drugs act on different processes; perhaps actin disruptors act by perturbing cortical actin to allow granules greater access to secretory sites, while filament enhancers act by some unrelated (and yet unknown) mechanism. (2) The two drugs act on a single process, both influencing GSIS by freezing the dynamic turnover of actin filaments. In the second case, we might expect inhibition of actin-related processes (actomyosin motors, endocytosis, filament branching, *et al.*) to phenocopy filament disruption. However, inhibition of Arp2/3 (actin branching) (9), Cdc42 (involved in actin rearrangements) (13), FAK (signals through focal adhesions) (14), and myosin II (primary actomyosin motor) (15) have all been shown to decrease GSIS in *ex vivo* islets or primary β cells, consistent with these proteins being involved in the normal secretion process. In contrast, the formin inhibitor SMIFH2 (which also inhibits myosins) (9) and an inhibitor of Rac1 slightly enhance GSIS from moue islets,

while the RhoA inhibitor rhosin dramatically enhances insulin secretion both at low and high glucose (13). Of course, these references encompass a variety of β cell models, as well as drug concentrations and treatment timing, which limits our ability to draw a unified model of this pathway.

Moving forward, a fuller understanding of actin's role in regulating insulin secretion will likely require live recordings of β cells with both actin and insulin granules clearly illuminated. This represents a significant technical challenge as insulin granules are so numerous (4000–14,000 per cell (16)) and packed so tightly as to make individual granules difficult to resolve with light microscopy. Even when a subset of granules is illuminated, identifying the extreme minority destined for secretion is a challenge. Advances in our understanding of β cell organization would help with overcome this challenge. Ma, *et al.* (2020) represent the vanguard of this effort, using two-photon imaging to query actin (Lifeact-GFP), insulin (proinsulin-GFP) and vesicle fusion events (sulforhodamine B). Yet even with this cutting-edge setup, they were unable to resolve actin filaments beyond the very bulkiest actin bands that underlie cell-cell boundaries. Trogden, *et al.* (2021) (17) used TIRF to explore the relationship between β cell microtubules and secretion events (marked by FluoZin-3). However, the narrower and much more densely packed actin filaments are unlikely to be clearly resolved in such a setup. Indeed, Wöllert and Langford (2022) resolved only a sparse network of large filaments using super-resolution TIRF-SIM applied to INS-1 cells, (18). The many smaller filaments that dominate the cortex and likely interact most directly with insulin granules remain obscured.

In summary, our data are not consistent with the long-standing model that cortical actin restricts the secretion of insulin granules. Clearly, the actin cytoskeleton is substantially involved in the mechanism of insulin secretion, as even short-term perturbation of actin filaments or actin-related proteins can have a dramatic effect on insulin secretion. However, the nature of the cytoskeleton's involvement remains unclear.

Experimental procedures

Cell culture

MIN6 cells (19) were cultured in high glucose DMEM (Gibco, #11965092) supplemented with 10% fetal bovine serum (FBS), 50 μM β-mercaptoethanol, and 100 U/ml penicillin-streptomycin (Gibco, #15140122). Over the course of use, cells were monitored at least weekly to ensure they still retained glucose-stimulated insulin secretion.

Rodent care and islet isolation

Rodent care was performed in strict accordance with protocols approved by the Washington University Institutional Animal Care and Use Committee (AALAC accreditation # D16-00245). C57BL/6J mice were acquired from Jackson Laboratories (Strain #000664) or bred on-site and had access to water and chow *ad libitum*. Islets were isolated from both male and female mice less than 12 months old. Under anesthesia (100 mg/kg ketamine; 20 mg/kg xylazine), pancreata

were surgically removed, then dissociated by shaking at 34 °C in HBSS (Gibco, #14025092) plus 0.75 mg/ml collagenase (Roche, #11213873001, dissolved at 12 mg/ml in HBSS without calcium – Gibco, #14175095) for 8 min, and washed three times in HBSS. Islets were picked manually under a stereomicroscope and allowed to recover overnight in RPMI 1640 (Gibco, #11879020) supplemented with 10% FBS, 11 mM glucose, and 100 U/ml penicillin-streptomycin.

Immunofluorescence

For immunofluorescence MIN6 cells were seeded onto uncoated #1.5 coverslips (Electron Microscopy Sciences, #72230-01), while islets were seeded onto the same coverslips coated with recombinant human laminin-521 (Gibco, #A29248, 0.5 μg/cm^2). Cells/islets were allowed to attach overnight, rinsed three times in KRBH (128.8 mM NaCl, 4.8 mM KCl, 1.2 mM KH$_2$PO$_4$, 1.2 mM MgSO$_4$, 2.5 mM CaCl$_2$, 10 mM HEPES, 5 mM NaHCO$_3$, 0.1% (w/v) bovine serum albumin (BSA), pH 7.4) plus 2.8 mM glucose, equilibrated in KRBH plus 2.8 mM glucose for 1 h, treated in KRBH with the indicated amount of glucose (11 mM for islets, 20 mM for MIN6 cells) and KCl (0 mM or 30 mM) for the indicated amount of time (2–15 min). At the end of the treatment time, samples were fixed for 30 min in 2% para-formaldehyde (diluted from 16% solution, Thermo Fisher Scientific, #28906) in phosphate-buffered saline (PBS, diluted from 10×, Corning, #46-013-CM). Fixed samples were rinsed three times in PBS, permeabilized in 0.1% Triton X-100 in PBS for 5 min, rinsed three times in BPS, and blocked for an hour with 2% BSA in PBS. After blocking, samples were stained with Phalloidin-AlexaFluor488 (Molecular Probes, #A12379) diluted in blocking buffer at 165 nM per the manufacturer's recommendation. Samples were then washed three times with PBS, then coverslips inverted onto a drop of ProLong Glass Antifade Mountant (Invitrogen, #P36980), and allowed to cure for 48 h before imaging.

All imaging was done on a Zeiss LSM880 laser-scanning confocal microscope using a Fluar 40× oil objective, numerical aperture 1.3, and a 32-PMT spectral detector array set to collect light from 495 nm to 630 nm. Images were taken at 1024 × 1024 pixels, a pixel dwell time of 1.03 μs, 2× line averaging, and a 2× zoom resulting in 0.1 μm per pixel. Images were processed in FIJI (ImageJ 1.53t), and graphed using GraphPad Prism (9.5).

F-:G-actin assessment

To assess the ratio of F-:G-actin, MIN6 cells were plated in a 24-well plate and allowed to adhere overnight. The next day, cells were equilibrated in KRBH plus 2.8 mM glucose for an hour, then treated for 5 min with KRBH +1 mM glucose, KRBH +20 mM glucose, or KRBH +20 mM glucose +30 mM KCl. Controls were treated for 30 min with KRBH +2.8 mM glucose +1 μM latrunculin B (Calbiochem, #428020) or 1 μM jasplakinolide (Millipore Sigma, #J4580). All samples were processed using the "G-actin/F-actin *In Vivo* Assay Kit" (Cytoskeleton Inc., #BK037) which involves lysing cells in a

filament-supporting buffer, pelleting filaments by ultracentrifugation (100,000*g*; 1 h), de-polymerizing filaments on ice, separating all by SDS-PAGE, and blotting for β-actin (buffers and antibody provided as part of kit). The secondary antibody was goat anti-mouse IRDye 800CW (LI-COR, #926-32210, used at 1:10,000). Blots were imaged on a LI-COR Odyssey M, and bands were analyzed with Image Studio Lite (5.2.5).

Scanning electron microscopy

Cells and islets were attached to coverslips and equilibrated in KRBH plus 2.8 mM glucose as in "Immunofluorescence" above. For images shown in Figure 2, the following equilibration samples were treated with KRBH plus 2.8 mM glucose, KRBH plus high (20 mM for MIN6, 11 mM for mouse islets) glucose, or KRBH plus high glucose and 30 mM KCl for 5 min. For those shown in Figure 4, samples were treated for 30 min with KRBH plus 2.8 mM glucose plus 1 μM cytochalasin D, 1 μM latrunculin B, 1 μM jasplakinolide, or an equal volume of the solvent DMSO (1 μl in 1 ml).

In all cases, cells were then quickly rinsed in warm HBSS, fixed, and extracted in PEM buffer (100 mM PIPES, pH 6.9; 1 mM EGTA; 1 mM $MgCl_2$) plus 2% Triton X-100 and 0.25% glutaraldehyde (prepared fresh the day of experiment; a new ampule of glutaraldehyde was used each time) for 5 min with gentle shaking, followed by 10 min in PEM buffer +2% Triton X-100 +1% (w/v) CHAPS with gentle shaking. Samples were then rinsed three times in PEM buffer and fixed in 0.15 M cacodylate buffer, pH 7.4 with 2% glutaraldehyde at 4 °C overnight.

Following fixation, coverslips were prepared for electron microscopy by treatment with 0.1% tannic acid for 20 min at room temperature, four rinses for 5 min each in water, 20 min in 0.2% aqueous uranyl acetate, three rinses for 10 min each in water, followed by a graded ethanol dehydration series with 5 min per step: 10%, 20%, 30%, 50%, 70%, 90%, 100%, 100%, 100%. Once dehydrated, samples were loaded into a critical point drier (Leica EM CPD 300) set to perform 12 CO_2 exchanges at the slowest speed. Samples were mounted on aluminum stubs with carbon adhesive tabs and coated with 5 nm each of carbon and iridium (Leica ACE 600). Prepared samples were imaged on a Zeiss Merlin FE-SEM using an InLens detector at 1.2 to 1.5 kV and 400 to 500 pA depending on the sample. Images were scanned at 1024 × 768 pixels, resulting in 11.16 nm per pixel at the 10,000× zoom shown in Figure 2.

Insulin secretion assay

For glucose-stimulated insulin secretion assays, MIN6 cells were plated in tissue-culture-treated 96-well plates and allowed to adhere overnight; mouse islets were plated on laminin-coated (0.5 μg/cm², as above) half-area 96-well plates, four islets per well and allowed to adhere overnight. On the day of the experiment, samples were washed three times in KRBH plus 2.8 mM glucose, then equilibrated in KRBH plus 2.8 mM glucose for 1 h. The equilibration sample was saved and replaced with a pre-treatment buffer containing KRBH plus 2.8 mM glucose plus inhibitors at the indicated concentrations (see below, "Inhibitors") for 30 min. Cells were then moved to a "secretion buffer" of KRBH plus high glucose (20 mM for MIN6; 11 mM for mouse islets) plus inhibitors at the indicated concentrations for 1 h. The secretion buffer was saved. Secretion and equilibration samples were spun at 1000*g* for 3 min to remove any cellular material and diluted as needed in KRBH to be within the range of detection of our insulin assay. Insulin in each sample was measured in technical duplicate using the Lumit Insulin Immunoassay (Promega, #CS3037A01, provided through Promega's early access program), with luminescence measured on a multimodal plate reader (Cytation5, BioTek). For MIN6 assays, three wells were assayed per condition; for islets (which have more variable size, composition, and signal) four wells were assayed per condition. Data were graphed using GraphPad Prism (9.5) and are shown throughout with a dot representing the insulin content in a given well's secretion buffer over the same well's equilibration buffer. Bar height represents the mean of the 3 to 4 wells measured in that condition. Error bars represent standard deviation.

Inhibitors

All inhibitors described here were dissolved in DMSO and stored as aliquots at −70 °C until the time of use. Latrunculin A (Millipore-Sigma, #L5163), latrunculin B (Calbiochem, #428020), cytochalasin B (Millipore-Sigma, #C6762), cytochalasin D (Millipore-Sigma, #C8273), swinholide A (Millipore-Sigma, #574776), jasplakinolide (Millipore-Sigma, #J4580). For glucose-stimulated insulin secretion assays, inhibitors were diluted into KRBH to the highest experimental concentration, then diluted with 1:10 serial dilutions in KRBH to make the remaining concentrations.

Data availability

Data required to assess our claims has been included in the manuscript where possible. We are happy to share raw images or data upon request to the corresponding author (DWP, piston@wustl.edu).

Abbreviations—The abbreviations used are: GSIS, glucose-stimulated insulin secretion; PBS, phosphate-buffered saline.

References

1. Chugh, P., and Paluch, E. K. (2018) The actin cortex at a glance. *J. Cell Sci.* **131**, jcs186254
2. Li, P., Bademosi, A. T., Luo, J., and Meunier, F. A. (2018) Actin remodeling in regulated exocytosis: toward a mesoscopic view. *Trends Cell Biol.* **28**, 685–697
3. Nightingale, T. D., Cutler, D. F., and Cramer, L. P. (2012) Actin coats and rings promote regulated exocytosis. *Trends Cell Biol.* **22**, 329–337
4. Asahara, S., Shibutani, Y., Teruyama, K., Inoue, H. Y., Kawada, Y., Etoh, H., *et al*. (2013) Ras-related C3 botulinum toxin substrate 1 (RAC1) regulates glucose-stimulated insulin secretion via modulation of F-actin. *Diabetologia* **56**, 1088–1097
5. Kalwat, M. A., Yoder, S. M., Wang, Z., and Thurmond, D. C. (2013) A p21-activated kinase (PAK1) signaling cascade coordinately regulates F-actin remodeling and insulin granule exocytosis in pancreatic β cells. *Biochem. Pharmacol.* **85**, 808–816
6. Bowe, J. E., Chander, A., Liu, B., Persaud, S. J., and Jones, P. M. (2013) The permissive effects of glucose on receptor-operated potentiation of insulin secretion from mouse islets: a role for ERK1/2 activation and cytoskeletal remodelling. *Diabetologia* **56**, 783–791
7. Naumann, H., Rathjen, T., Poy, M. N., and Spagnoli, F. M. (2018) The RhoGAP Stard13 controls insulin secretion through F-actin remodeling. *Mol. Metab.* **8**, 96–105
8. Wang, B., Lin, H., Li, X., Lu, W., Kim, J. B., Xu, A., *et al*. (2020) The adaptor protein APPL2 controls glucose-stimulated insulin secretion via F-actin remodeling in pancreatic β-cells. *Proc. Natl. Acad. Sci. U. S. A.* **117**, 28307–28315
9. Ma, W., Chang, J., Tong, J., Ho, U., Yau, B., Kebede, M. A., *et al*. (2020) Arp2/3 nucleates F-actin coating of fusing insulin granules in pancreatic β cells to control insulin secretion. *J. Cell Sci.* **133**, jcs236794
10. Orci, L., Gabbay, K. H., and Malaisse, W. J. (1972) Pancreatic beta-cell web: its possible role in insulin secretion. *Science* **175**, 1128–1130
11. Mourad, N. I., Nenquin, M., and Henquin, J.-C. (2013) Amplification of insulin secretion by acetylcholine or phorbol ester is independent of β-cell microfilaments and distinct from metabolic amplification. *Mol. Cell. Endocrinol* **367**, 11–20
12. Nevins, A. K., and Thurmond, D. C. (2003) Glucose regulates the cortical actin network through modulation of Cdc42 cycling to stimulate insulin secretion. *Am. J. Physiol. Cell Physiol.* **285**, C698–C710
13. Ng, X. W., Chung, Y. H., Asadi, F., Kong, C., Ustione, A., and Piston, D. W. (2022) RhoA as a signaling hub controlling glucagon secretion from pancreatic alpha-cells. *Diabetes* **71**, 2384–2394
14. Jevon, D., Deng, K., Hallahan, N., Kumar, K., Tong, J., Gan, W. J., *et al*. (2022) Local activation of focal adhesion kinase orchestrates the positioning of presynaptic scaffold proteins and Ca2+ signalling to control glucose dependent insulin secretion. *Elife* **11**, e76262
15. Arous, C., Rondas, D., and Halban, P. A. (2013) Non-muscle myosin IIA is involved in focal adhesion and actin remodelling controlling glucose-stimulated insulin secretion. *Diabetologia* **56**, 792–802
16. Müller, A., Schmidt, D., Xu, C. S., Pang, S., D'Costa, J. V., Kretschmar, S., *et al*. (2021) 3D FIB-SEM reconstruction of microtubule-organelle interaction in whole primary mouse β cells. *J. Cell Biol.* **220**, e202010039
17. Trogden, K. P., Lee, J., Bracey, K. M., Ho, K.-H., McKinney, H., Zhu, X., *et al*. (2021) Microtubules regulate pancreatic β-cell heterogeneity via spatiotemporal control of insulin secretion hot spots. *Elife* **10**, e59912
18. Wöllert, T., and Langford, G. M. (2022) Super-resolution imaging of the actin cytoskeleton in living cells using TIRF-SIM. In: Gavin, R. H., ed. *Cytoskeleton: Methods and Protocols*, Springer US, New York, NY: 3–24
19. Miyazaki, J., Araki, K., Yamato, E., Ikegami, H., Asano, T., Shibasaki, Y., *et al*. (1990) Establishment of a pancreatic beta cell line that retains glucose-inducible insulin secretion: special reference to expression of glucose transporter isoforms. *Endocrinology* **127**, 126–132

SSASBMB